

Graph Neural Networks with Precomputed Node Features

Beni Egressy¹ Roger Wattenhofer¹

Abstract

Most Graph Neural Networks (GNNs) cannot distinguish some graphs or indeed some pairs of nodes within a graph. This makes it impossible to solve certain classification tasks. However, adding additional node features to these models can resolve this problem. We introduce several such augmentations, including (i) positional node embeddings, (ii) canonical node IDs, and (iii) random features. These extensions are motivated by theoretical results and corroborated by extensive testing on synthetic subgraph detection tasks. We find that positional embeddings significantly outperform other extensions in these tasks. Moreover, positional embeddings have better sample efficiency, perform well on different graph distributions and even outperform learning with ground truth node positions. Finally, we show that the different augmentations perform competitively on established GNN benchmarks, and advise on when to use them.

1. Introduction

Given the impressive success of neural networks in the text and image domains, recently research has also turned its attention to graph-structured data. In just a few years there has been explosive interest in the area, with Graph Neural Networks (GNNs) achieving state-of-the-art results in a wide range of applications, including molecule recognition, physics simulations, recommendation systems, fake news detection and social networks (Fout, 2017; Sanchez-Gonzalez et al., 2020; Ying et al., 2018).

Most GNN architectures are based on the message passing framework, which can be summarized in three main steps: (1) node representations are initialized with their initial features (if available) or node degrees (if not available); (2) nodes update their representations by aggregating the representations of neighboring nodes; (3) the final representations of nodes are combined in a readout layer to solve the task at hand.

Although this framework has been a recipe for success, it has also been observed that such GNNs are limited in their

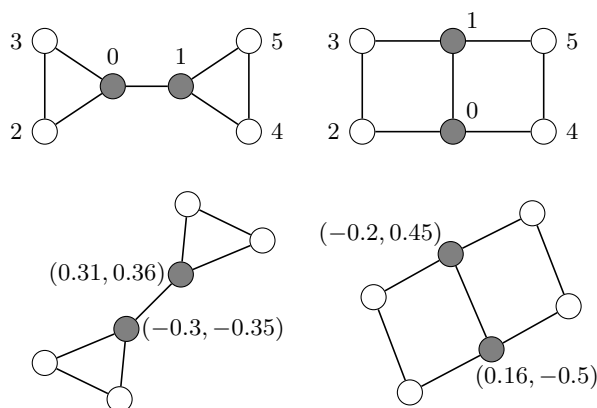


Figure 1. Example of limitation of WLGNs, which cannot distinguish the graphs on left and right without node features. Both our augmentations, canonical ID (above) and positional embedding (below) resolve this issue. For example the two nodes with canonical ID 0 (top) now have different 1-hop neighborhoods (1, 2, 3 vs 1, 2, 4) and can be distinguished by 2 rounds of message passing. For the positional embeddings, we only show the coordinates of select nodes, but the positions correspond to the embeddings.

power to distinguish even very simple graphs, e.g., see Figure 1 (top, ignoring the labels). This has been formalized by proving that message-passing GNNs are upper-bounded by the Weisfeiler-Lehman (WL) isomorphism test (Weisfeiler & Leman, 1968; Xu et al., 2018; Morris et al., 2019). We shall refer to such GNNs as Weisfeiler-Lehman GNNs, or WLGNs.¹ More precisely, WLGNs produce identical representations for (sub-)graphs that the WL test fails to distinguish. In particular these include regular graphs, where nodes cannot be distinguished based on their degree and the degree of the nodes around them.

As a consequence there have been various suggestions to overcome the expressive limit of WLGNs. These include: breaking symmetries by making perturbations to the input graph; using higher-order representations of the input graph; and initializing the nodes with additional features.

The latter approach will be the focus of this paper. We explore the power of GNNs augmented with precomputed node features. Since initializing node representations is the

¹We use the term WLGNs as used in (Li et al., 2020)

first main step of most standard GNNs, this approach can be combined with many different architectures.

Our main contributions are:

- We propose several new augmentations for standard GNN architectures to improve their expressive power beyond the WL test: canonical node IDs, l_∞ embeddings, positional embeddings, random bits, and combinations of the above. See Figure 1.
- For several augmentations, we formally prove that they make appropriate GNN architectures universal.
- We conduct extensive subgraph detection tests on carefully constructed benchmark datasets to show the empirical validity of these augmentations.
- We show that the augmentations perform competitively on established benchmarks.

2. Preliminaries

2.1. Notation

We consider unweighted, undirected, connected graphs $G = (V, E)$ consisting of $n = |V|$ nodes. We denote an edge between nodes u and v by e_{uv} . We denote the neighborhood of node v by $N(v) = \{u \in G \mid e_{uv} \in E\}$, the degree of node v by $\deg(v) = |N(v)|$, and the maximum degree of all nodes by $\Delta = \max_{v \in V} \deg(v)$. The graph diameter D is the length of the longest shortest path between any two nodes.

2.2. GNNs

Most GNN architectures are based on the message passing framework, which consists of: (1) node initialization, (2) node updates via message passing, and (3) a readout step. The message passing itself is conducted in rounds. In each round there are three steps. First, every node creates a MESSAGE based on its current embedding. It then sends this message to each of its neighbors. Second, when the nodes have received messages from each of their neighbors, they AGGREGATE these messages. Finally they UPDATE their state by combining their current state with the aggregate embedding they have just calculated. One round of message passing corresponds to one layer of a GNN. Usually k layers are stacked on top of each other so that after k rounds of message passing each node will have received information, either directly or indirectly, from all of the nodes in its k -hop neighborhood. Usually, MESSAGE, AGGREGATE, UPDATE and READOUT are functions with learnable parameters, and they are shared among all the nodes. In the simple case, where the messages are the current state of the node, the

GNN can be summarized as follows:

$$\begin{aligned} h_v^{(0)} &= x_v \\ a_v^{(t)} &= \text{AGGREGATE}(\{h_u^{(t-1)} \mid u \in N(v)\}) \\ h_v^{(t)} &= \text{UPDATE}(h_v^{(t-1)}, a_v^{(t)}) \\ y_v &= \text{READOUT}(h_v^{(t)}) \end{aligned}$$

where x_v are the initial node features and $h_v^{(t)}$ is the embedding vector, or representation, of node v after t rounds of message passing. The readout layer above is a function of a single node in the case of node classification, but could also be a function of all the nodes (graph classification), or a subset of the nodes (link prediction).

Since reordering the nodes of a graph does not change the underlying topology, in general we want to learn a graph or node function that is invariant to permutations of the nodes. This is commonly ensured by treating incoming messages as a set (or multiset) and learning a (permutation-invariant) set aggregation function for AGGREGATE.

2.3. Weisfeiler-Lehman Test

The message passing framework is closely related to the Weisfeiler-Lehman (WL) isomorphism test. The WL test is an iterative color refinement procedure (Weisfeiler & Leman, 1968; Shervashidze et al., 2011). Each node keeps a state (or color) that gets refined in each iteration by aggregating information from the neighbors’ states and combining it with its own.

More precisely, in each iteration we assign to each node a tuple containing the node’s state and a multiset of the node’s neighbors’ states. Then we hash these tuples to give each node its new state. In this way all nodes with different tuples receive different new states and all nodes with the same tuple receive the same new state. In particular two nodes with different states at time $T \geq 0$ will never have the same state after time T ; hence we call this a *refinement* algorithm. All nodes are assigned the same initial state, so for example, after the first iteration the state of a node corresponds to its degree. To check whether two graphs are isomorphic we can run this procedure on both graphs until convergence and then compare the multisets of the final node states. If they are different, then the graphs are not isomorphic. If they are the same, then we cannot be sure.

If the WL test cannot distinguish two graphs, then a standard message-passing GNN cannot distinguish them either: intuitively, the nodes in the two graphs receive the same messages and create the same embeddings in each round, and thus they always arrive at the same final result. As such, a message-passing algorithm can only be as powerful² as the WL algorithm. In fact for some GNNs, it can be shown

²as good at distinguishing non-isomorphic graphs

that they are exactly as powerful as the WL isomorphism test. This is the case with GIN (Xu et al., 2018), which we shall rely on in this paper.

The WL test can be extended to start with an initial labelling of the nodes. If the nodes have initial features, then these can be hashed to give the initial states before continuing the algorithm. Similarly, initial features can be used to increase the power of a GNN. For example, in chemistry problems, the nodes might represent atoms of a molecule, and so the type of atom would be an initial feature for each node (Irwin et al., 2012; Yanardag & Vishwanathan, 2015).

2.4. Distributed Computing Models

The GNN message passing framework is also closely related to message passing models in distributed computing³.

As GNNs, distributed computing deals with a network of nodes, connected by message passing edges, and the task is to calculate some function of the graph. As GNNs, all nodes also execute the same algorithm; however, the algorithm is designed rather than learned.

One major difference to GNNs is that in distributed computing, the nodes usually have unique IDs.⁴ This ensures that a node can always distinguish its neighbors and indeed all nodes in the graph. If computation and communication is unbounded, any problem can be solved in D rounds of message passing, where D is the diameter of the graph. Each node can simply encode all the information it has about the graph so far into a message and send this information to all of its neighbors in every round. With the help of the unique IDs, after D rounds, every node will know the exact topology of the graph.

3. Motivation

Upon considering the aforementioned distributed computing model, one natural way to increase the power of GNNs is to treat the node indices as node IDs and use the one-hot encoding of node indices as an input feature. This way the GNN can distinguish all the nodes, and it can theoretically distinguish all non-isomorphic graphs, making it “universal”. However, the embedding will depend heavily on the initial ordering of the vertices, and there are $n!$ possible permutations. As such the GNN loses its inductive advantage of mapping nodes with identical neighborhoods to the same embedding, resulting in a great loss in generalization ability. Similarly, one could use random features as input node features (Abboud et al., 2020;

³The connection between GNNs and distributed computing models was first noted in (Loukas, 2019).

⁴There are exceptions, in particular anonymous networks (Emek et al., 2014).

Sato et al., 2021). This can also be proven to give “universal” GNNs, but it also leads to the same generalization problems. Basically, we want to give each node a label such that:

- (a) the probability to have the same label(s) is high if the graph is the same, and
- (b) the probability to have the same label(s) is low if the graph is not the same.

Using no labels (or identical labels), as in the WL algorithm, perfectly achieves (a), but does not do well regarding (b), since many graphs remain indistinguishable. On the other hand, using node indices or random features as labels may achieve “universality” (b), but does less well regarding (a). The problem is that the additional information is not permutation invariant. As a consequence, exponentially more training examples might be needed. The additional information can also confuse the learning procedure, and the GNN may weigh the additional information too heavily in the decision process.

We hypothesise that the right balance of (a) and (b) is at the core of a deeper understanding of GNNs. By keeping the additional information low, we get a net benefit from adding it. We explore this hypothesis by testing different augmentations aimed at balancing (a) and (b).

First, we propose adding a vector of random bits. By controlling the length of the vector we have a fine grained control over (a) and (b). Second, we propose precomputed *canonical node IDs*; these do not burden the learner with an exponential input diversity, while at the same time offering benefits regarding (b).

The most impressive results are obtained by our novel precomputed *positional node embeddings*. Like random features, these geometric labels also fulfill (b) to a sufficient degree. While positional embeddings add even more information than node IDs, in practice GNNs can interpret positional coordinates well. GNNs seem to develop an understanding of these coordinates (e.g., the distance between two positions), without being distracted by the erratic raw values of the positions.

3.1. Canonical node IDs

Canonical node IDs are node IDs that are standardized such that all the nodes in a graph always receive the same IDs however the nodes are permuted at the input. It is not clear how we can find canonical node IDs fast in practise. Indeed, an algorithm that produces canonical node IDs also solves the graph isomorphism problem, and until recently it was not known whether the graph isomorphism problem can be solved in sub-exponential time. However, Babai et al. showed that solving graph isomorphism and finding a

canonical form can be done in quasipolynomial time (Helfgott et al., 2017; Babai, 2019). However, their approach is mostly of academic interest, since in practice the overhead is too high. Instead, NAUTY (McKay & Piperno, 2014) and BLISS (Junttila & Kaski, 2007) are used in practice. These algorithms do not guarantee a sub-exponential runtime, but are fast in practice. We will use NAUTY when calculating canonical orderings in this paper. See Figure 1 for example graphs with canonical IDs.

First we show that GNNs with canonical node IDs can theoretically distinguish any two non-isomorphic graphs. The proof follows from Corollary 3.1 in (Loukas, 2019). As such we leave the proof for the appendix.

Theorem 3.1. *GIN of sufficient depth augmented with canonical node IDs can distinguish any two non-isomorphic graphs.*

In our empirical tests, we use the one-hot encoding of the canonical node IDs as initial node features. Note that using canonical node IDs is very similar to using the node indices as features. But crucially there are no longer $n!$ possible inputs for the same graph. Instead a graph will always receive the same labelling. We expect this to lead to better learning and sample efficiency.

3.2. Positional node Embeddings

There have been recent attempts to improve GNNs by learning positional embeddings, see for example (Ma et al., 2021) and (Klemmer et al., 2021). However, these are based on solving some auxiliary task while training the main network, with the former using a combined neural network, and the latter focusing on geographic data.

Using precomputed positional node embeddings has several potential advantages over learned embeddings. Firstly, the node embedding algorithms we use in this paper take the whole graph topology into account. This allows them to differentiate nodes that have the same local neighborhoods. Of course, one could also use fully connected message passing to achieve this. But message passing GNNs have a known problem with oversmoothing and fully connected layers would only exaggerate this problem. GNNs with precomputed node features do exacerbate this issue, as nodes still aggregate messages from their neighbors rather than being flooded by information from the whole graph. Finally, precomputed node features are also very versatile; the node features can be used to augment any standard GNN.

l_∞ -EMBEDDINGS

We propose embedding the input graph into l_∞ and using the locations as node features. We begin by showing that any graph can be embedded into l_∞ isometrically (i.e., such that all shortest path distances are preserved). If we

have an embedding that preserves all the distances, then no information about the graph is lost. One could throw away the graph topology and the set of embeddings would still hold all the information.

Theorem 3.2. *Every graph $G = (V, E)$ embeds isometrically into l_∞ .*

See the appendix for a proof. Unfortunately the embedding in the proof uses n dimensions, and adding node features of length n is impractical for large graphs. It can be shown that $\Theta(n)$ is in fact a lower bound for the dimension of isometric embeddings into l_∞ (Coppersmith, 2001). For other l_p spaces, isometric embeddings are not even possible.

We use the isometric l_∞ -embeddings from the proof in our synthetic tasks. These graphs are small enough for this approach to be practical. Moreover, we can prove that GNNs with l_∞ -embeddings are “universal”. The proof follows the same approach as Theorem 3.1, see appendix.

Theorem 3.3. *GIN of sufficient depth augmented with isometric l_∞ -embeddings can distinguish any two non-isomorphic graphs.*

Although these embeddings do not lose any information about the graph, there is a major drawback. The embeddings are large and their dimension depends on the number of nodes, so if we want our model to work for train or test graphs of up to n nodes, then we need to use labels of length n . This is not only inconvenient, but makes the learning problem much harder. As an alternative we introduce approximate Euclidean embeddings.

POSITIONAL EMBEDDINGS

To calculate our positional embeddings we use a force-directed technique based on an approach proposed in (Kamada et al., 1989). The main idea is to obtain a layout of the graph minimizing the following STRESS function:

$$\text{STRESS}(P) = \sum_{i < j} w_{ij} (\|p(v_i) - p(v_j)\|_2 - d_{ij})^2,$$

where $p(v_i)$ is the coordinate position of vertex v_i in the Euclidean vector space; d_{ij} is the shortest path distance between nodes v_i and v_j ; and w_{ij} is a weighting factor for balancing the influence of certain pairs of nodes. We use $w_{ij} = d_{ij}^{-2}$. The localized Newton-Raphson method is used to optimize the stress function. This is an iterative solver, where in each step a single node is chosen and the standard N-R method is used to find a local minimum of the stress function. See Figure 1 for example graphs with labels.

One can think of this approach as placing an ideal spring between every pair of nodes with length equal to the shortest

path distance between the endpoints. The springs are then used to push/pull the nodes so that their euclidean distance approximates their shortest path distance in the graph.

These algorithms are randomized so they do not produce the same embeddings when run multiple times⁵. However, the relative positions between nodes are always optimized. Intuitively, this is something that should help with generalization to unseen graphs. Regardless of the exact placement of nodes, relative distances should be preserved. Unlike random features or canonical node labels, relative positions encode structural information about the nodes.



Figure 2. Example graphs that cannot be embedded into Euclidean space (of any dimension).

In general, unlike with the l_∞ space, graphs cannot always be isometrically embedded into the euclidean space, see Figure 2. Moreover there can be optimum solutions (with lowest STRESS), where different nodes receive the same position. This means that we cannot apply the same universality result that we used in Theorem 3.1, and the associated augmented GNNs are no longer universal function approximators. This is highly unlikely in multiple dimensions.

3.3. Random Baselines

Using random node features to initialize GNNs was first explored in (Sato et al., 2021), and was shown to give universal function approximators in (Abboud et al., 2020). In the latter, uniform and normal distributions, and in the former discrete uniform distributions are used to initialize the nodes. We initialize our random features in three different ways:

Random Gaussian: In this model, we add a vector of d random Gaussian samples to each node. The samples are generated i.i.d., from a $\mathcal{N}(0, 1)$ distribution. This is similar to (Abboud et al., 2020). We denote this as $rNormal(d)$.

Random Uniform Integer: In this model, we assign a random integer from 0 to 99 to each node; denoted $rUniform$.

Randombits: In this model, we add a vector of d random bits to each node. The random bits are generated i.i.d., from a Bernoulli(0.5) distribution. We denote this as $rBits(d)$.

Note that random features can be viewed as a form of training data augmentation. We generate the features freshly

⁵We run the embedding algorithm a single time for each training and test graph, and thereafter keep these embeddings fixed during training.

each time an input graph is presented to the model. As such the model sees many versions of the same training graph. This could be an advantage over the precalculated canonical and positional node features.

3.4. Our Model

First we precalculate the additional node features for a given input graph, be they canonical node IDs, positional node embeddings, or random features. We then concatenate the precalculated node features with the provided node features (if available) and use these as input for our GNN. We mainly use the GIN architecture for consistency (Xu et al., 2018). We choose GIN as it can be shown to be theoretically as powerful as the WL test.

4. Experiments

4.1. Model Parameters

Unless otherwise stated, we use GIN as our standard WL-GNN. We use 5 layers by default with hidden dimension 64. We use weighted cross-entropy loss, Adam optimizer with initial learning rate 0.01 and decay of rate 0.5 after every 50 epochs. We use dropout on the final layer and we train for 300 epochs by default with a batch size of 32.

4.2. Datasets beyond WL

To systematically test the practical expressiveness of GNNs with the suggested node features, we propose a series of binary node classification tasks on regular graphs. The model is tasked with detecting a particular subgraph in the input, and outputting 1 for all nodes that are in such a subgraph, and 0 for all nodes that are not in such a subgraph. Since the graphs are regular, the tasks cannot be solved by standard WL-GNNs; indeed all nodes look identical to the WL test.

Ci_N: We generate N regular train and N regular test graphs, with ground truth labels indicating whether a node is in a cycle of length i . This synthetic task is based on C3_1000 from (Sato et al., 2021). The degree we use for generating these regular graphs is given by the degree that leads to the closest-to-even split of ground truth labels.⁶

Ki_N: We generate N train and N test graphs, with ground truth labels indicating whether a node is in a clique of size i .

LCC_N: We generate N train and N test graphs, with ground truth labels indicating how many triangles a node is in. See (Sato et al., 2021).⁷

⁶An exception to this is C3_1000, where we use degree 3 (instead of 4) to match the degree from (Sato et al., 2021).

⁷LCC, or local clustering coefficient, of a node in a graph quantifies how close its neighbors are to being a clique. This is given by the number of triangles divided by the number of potential triangles based on the number of neighbors. Here we do

model	C3	C4	C5	C6	K4	K5	K6	LCC
GIN	0.500	0.500	0.500	0.500	0.500	0.500	0.500	0.500
+canon(20)	0.943	0.605	0.544	0.560	0.673	0.594	0.577	0.843
+ l_∞ (20)	0.686	0.597	0.526	0.548	0.598	0.562	0.536	0.701
+pos(2)	0.968	0.910	0.763	0.723	0.780	0.751	0.752	0.880
+pos(2)+rBits(1)	0.968	0.910	0.773	0.722	0.783	0.755	0.758	0.884
+rUniform(1)	0.913	0.675	0.593	0.598	0.551	0.519	0.514	0.686
+rNormal(1)	0.898	0.652	0.587	0.609	0.553	0.512	0.508	0.685
+rBits(2)	0.949	0.701	0.612	0.622	0.546	0.507	0.515	0.695
ppgn* (Maron et al., 2019)	0.707	0.742	0.667	0.623	0.629	0.651	0.706	0.645
dropggn (Papp et al., 2021)	0.665	0.671	0.671	0.624	0.655	0.675	0.658	0.660

Table 1. AUROC scores on the synthetic tasks using GIN with 5 layers as the base GNN model. Model name indicates the node feature used to augment the base model, with numbers in brackets indicating the size of the additional node features. All models were run with the same hyperparameter settings (epochs, learning rate, dropout, etc.). *Ppgn had to be adapted for node classification.

Note that we do not discard any randomly generated graphs based on the number of 0 and 1 labels. This ensures that our datasets do not have any prior biases resulting from the generation process. They come from the uniform distribution over all connected regular graphs of given degree with given size. Also note that this means that the GIN test accuracy baseline (with no additional node features) is given by the *max* of the proportion of 0’s and 1’s. However the weighted AUROC (Area Under the Receiver Operating Characteristic Curve) baseline for WLGNs is 0.5. As such we will generally quote weighted AUROC scores, following (Sato et al., 2021). Please check the appendix for the accuracy scores.

We ran all our augmentations individually and we combined the top two augmentation (positional embeddings and random bits) by concatenating the features. All GIN based models were run with the same hyperparameter settings. We compare against ppgn (Maron et al., 2019) and the recent DropGNN (Papp et al., 2021), both of them models specifically designed to go beyond the WL test. We adapted ppgn for node classification, as it was implemented as a graph classification model. See Table 1 for the results. Most notable is that the positional embeddings outperform all the alternatives on all the datasets. We ran the same experiments with GCN (Kipf & Welling, 2016) as our base model and got similar results, see appendix.

4.3. Effect of Embedding Dimension

We experiment with using larger embedding spaces for the positional embeddings. Additional dimensions allow for better separation of the nodes; this can be particularly advantageous for dense graphs. However, we find that 2-dimensional embeddings perform the best across the synthetic tasks. See Figure 3 for results on C3.

not divided by the number of potential triangles, so the labels are just a triangle counts.

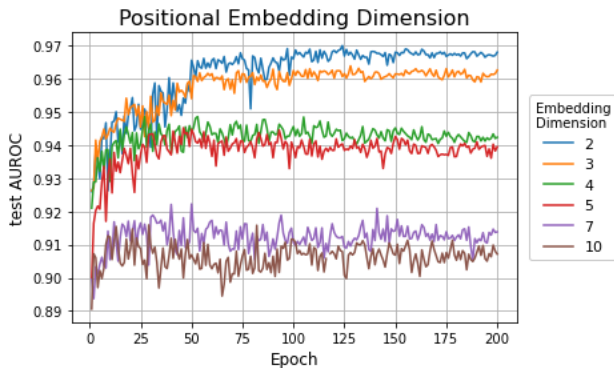


Figure 3. Weighted test AUROC scores for different positional embedding dimensions. Results for C3 task.

4.4. Investigating Learning Efficiency

As noted in our description, we expect GNNs with canonical IDs to have a better learning efficiency, because the nodes of an input graph will always receive the same IDs. This is in contrast to the random augmentations. To confirm this, we plot the training loss per epoch for C3_1000 in Figure 4. We see that the training loss for the model with canonical IDs drops the fastest and levels off the soonest. The model with positional node embeddings levels off next and the random augmentations level off last. See the appendix for a similar plot of the test AUROC.

4.5. Investigating Sample Efficiency

The models utilizing positional node embeddings perform significantly better on all the synthetic tasks with the limited training data (N=1000). This suggests that positional node embeddings, although not necessarily consistent between isomorphic graphs, store graph topological data in a somewhat consistent and generalizable way. Since neighboring nodes are placed closer together, it becomes possible to check whether two neighbors are themselves connected

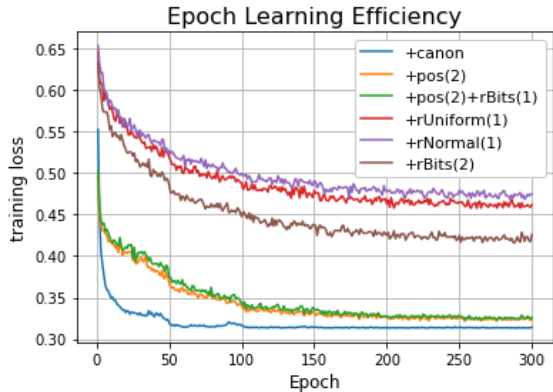


Figure 4. Training loss over the first 300 epochs on C3.

based on their positions. This, at least intuitively, might explain why GNNs with positional node embeddings are dramatically better at finding small cycles and cliques in regular graphs.

As we increase the training data available, the GNN with one-hot canonical node labels eventually ends up overtaking even the GNNs with positional node embeddings for the smaller cycle detection tasks, C3 and C4. We show results for C4 in Table 2. On all other synthetic tasks, the positional node embeddings still outperform the alternatives.

model	C4.1000	C4.2000	C4.4000	C4.8000
GIN	0.500	0.500	0.500	0.500
+canon(20)	0.624	0.645	0.794	0.970
+ l_∞ (20)	0.577	0.598	0.624	0.635
+pos(2)	0.904	0.932	0.945	0.949
rUniform(1)	0.669	0.673	0.677	0.669
rNormal(1)	0.669	0.665	0.666	0.667
rBits(2)	0.689	0.708	0.696	0.709

Table 2. Weighted AUROC scores with different training dataset sizes on the C4 cycle detection task.

4.6. Effect on Other Graph Distributions

We check that the higher expressivity of our model with positional embeddings does not come at the cost of lower accuracy on other graph distributions, where standard GNNs already perform well. We repeat the synthetic tasks with Erdős-Renyi graphs in place of regular graphs. A graph is constructed by initializing n nodes and connecting every pair of nodes independently with probability p . We choose p separately for each task so as to balance the ground truth labels of the dataset. The results can be seen in Figure 5.

We see that in most tasks, the model with random bits achieves the highest test accuracy. However the other models do not perform much worse. In particular, the model using positional embeddings also performs similarly

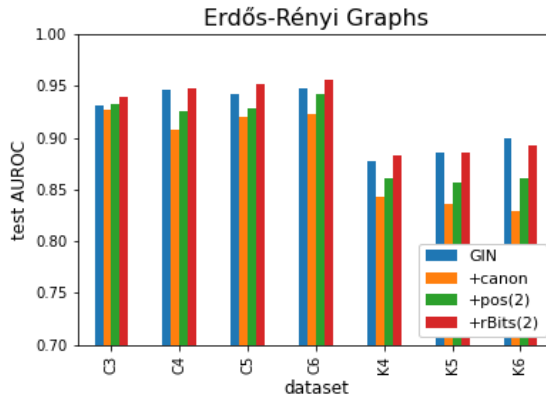


Figure 5. Weighted test AUROC on Erdős-Rényi graphs.

to using no additional node features.

4.7. Positional Embeddings vs Ground Truth Positions

To compare the positional embeddings with ground truth positions, we generate unit disk graphs in the two dimensional euclidean plane. We select 20 points in the unit square uniformly at random and connect nodes that are within a certain threshold distance to give us our graph. The threshold distance is chosen per task so as to keep the classes balanced. We augment the GNN with ground truth positions and compare against using our own positional embeddings.

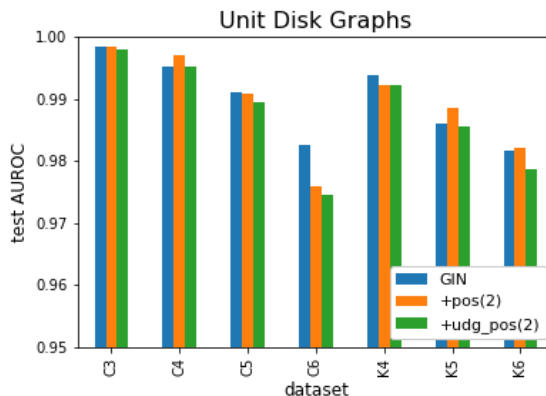


Figure 6. Weighted test AUROC on unit disk graphs.

The results can be seen in Figure 6. The positional embeddings perform better than the ground truth positions in almost every task. In several tasks the standard GNN performs the best. This indicates that unit disk graphs can be distinguished by standard GNNs with a high probability.

4.8. Benchmark Datasets

We evaluate our augmented GIN models on real-world graph classification datasets. We compare against the original GIN architecture and various GNN models that aim to go beyond the WL test. We consider four bioinformatics datasets (MU-

GNNs with Precomputed Node Features

dataset	MUTAG	PTC	PROTEINS	NCI1	COLLAB	IMDBBINARY	IMDBMULTI	REDDITBINARY
size	188	344	1113	4110	5000	1000	1500	2000
classes	2	2	2	2	3	2	3	2
avg node count	17.9	25.5	39.1	29.8	74.4	19.7	13	429.6
WL subtree (Shervashidze et al., 2011)	90.4 ± 5.7	59.9 ± 4.3	75.0 ± 3.1	86.0 ± 1.8	78.9 ± 1.9	73.8 ± 3.9	50.9 ± 3.8	81.0 ± 3.1
Invariant Graph Networks (Maron et al., 2018)	83.89±12.95	58.53±6.86	76.58±5.49	74.33±2.71	78.36±2.47	72.0±5.54	48.73±3.41	NA
GIN (Xu et al., 2018)	89.4±5.6	64.6±7.0	76.2±2.8	82.7±1.7	80.2±1.9	75.1±5.1	52.3±2.8	92.4 ± 2.5
1-2-3 GNN (Morris et al., 2019)	86.1±	60.9±	75.5±	76.2±	NA	74.2±	49.5±	NA
ppgn (Maron et al., 2019)	90.55±8.7	66.17±6.54	77.2±4.73	83.19±1.11	80.16±1.11	72.6±4.9	50±3.15	NA
DropGNN (Papp et al., 2021)	90.4 ± 7.0	66.3 ± 8.6	76.3 ± 6.1	NA	NA	75.7 ± 4.2	51.4 ± 2.8	NA
GIN*	89.33±5.6	63.65±11.2	73.68±3.7	82.24±1.3	78.00±2.1	74.90±2.9	51.20±2.8	89.95±1.6
+canon(20)	86.14±7.2	61.89±4.2	70.81±4.8	67.42±2.2	74.22±1.9	69.30±3.9	47.13±2.9	79.25±4.3
+pos(2)	83.51±5.2	61.39±7.7	74.21±3.6	74.40±2.5	74.70±1.9	70.60±3.0	49.60±3.8	89.15±2.0
+pos(2)+rBits(1)	86.67±6.3	59.04±7.3	73.76±3.7	74.96±1.6	75.20±1.3	71.50±2.5	50.67±3.3	89.00±1.6
+rBits(2)	89.80±7.9	65.10±8.3	75.38±3.8	81.73±2.0	76.10±2.2	75.30±3.6	51.87±2.3	90.60±2.1

Table 3. Test accuracies and standard deviations on the benchmark tasks. *We include scores for our base GIN model for consistency; these are slightly lower than the official values. We highlight the best augmentation and the best overall model.

TAG, PTC, PROTEINS, NCI1) and four social network datasets (COLLAB, IMDB-BINARY, IMDB-MULTI, REDDITBINARY) (Yanardag & Vishwanathan, 2015).

We follow the experimental setup from the original GIN paper (Xu et al., 2018). For the social network datasets we use the node degree as the input feature and for the bioinformatics datasets we use the categorical node features supplied with the graphs. We report the 10-fold cross-validation accuracies, with mean and standard deviation (Yanardag & Vishwanathan, 2015). We use the original 5-layer GIN model (4 layers + input layer) and we apply the most promising augmentations from our synthetic experiments.

Out of the different augmentations, random bits preforms the best on most of the benchmark datasets, outperforming also the base model without additional node features. The augmentations are not state of the art, but they perform competitively on all the tasks. Given how well the WL subtree baseline performs on the datasets, it is possible that classifying graphs in this dataset rarely requires higher expressiveness. As such there is little added value in our augmentations elevating GIN beyond the WL barrier. This is also the case for the other expressive GNNs.

5. Related Work

The first works applying neural networks to graphs used recurrent neural networks to learn node representations (Gori et al., 2005; Scarselli et al., 2008). Afterwards many works drew on the success of convolutional neural networks (Krizhevsky et al., 2012) and generalized this approach to graphs (Henaff et al., 2015; Kipf & Welling, 2016; Hamilton et al., 2017; Veličković et al., 2017). Many of these approaches were later shown to fit into the same general framework of message passing neural networks (Gilmer et al., 2017). In turn this whole framework was shown to be related to, and indeed upper-bounded by the WL isomorphism test. Although the WL test can distinguish graphs

with a very high probability, it has some notable blind spots such as detecting cycles in regular graphs.

In an effort to overcome this boundary, there have been many proposals for increasing the expressive power of GNNs. These include: adding port numbers to edges (Sato et al., 2019), adding random features (Sato et al., 2021; Abboud et al., 2020), randomly dropping nodes or edges (Papp et al., 2021; Rong et al., 2019), adding subgraph counts (Bouritsas et al., 2020), or mimicking higher order WL tests (Maron et al., 2019; Morris et al., 2019). But many of these either still fail to distinguish simple graphs or are prohibitively expensive.

Positional encodings also play a major role in NLP. The current state-of-the-art NLP models are based on the permutation invariant attention mechanism (Devlin et al., 2018; Lewis et al., 2019). But since the relative positions of words is of great importance to meaning, positional embeddings are added to the input tokens to indicate order (Shaw et al., 2018).

6. Conclusion

We find that positional node embeddings can be very effective for subgraph detection, and can learn to generalize with limited training data. They should be used in applications where subgraph detection is critical, or where the data has inherent spatial meaning. Canonical node IDs will be more useful in applications with plenty of data. Random bits can be useful in any scenario and clearly outperform more noisy random features. They can be considered both for increasing expressivity in WL blind spots, and as a form of data augmentation. One could also consider using additional node features only for the “difficult” cases. These could be identified by running a WL test before applying a GNN.

References

- Abboud, R., Ceylan, I. I., Grohe, M., and Lukasiewicz, T. The surprising power of graph neural networks with random node initialization. *arXiv preprint arXiv:2010.01179*, 2020.
- Babai, L. Canonical form for graphs in quasipolynomial time: preliminary report. In *Proceedings of the 51st Annual ACM SIGACT Symposium on Theory of Computing*, pp. 1237–1246, 2019.
- Bouritsas, G., Frasca, F., Zafeiriou, S., and Bronstein, M. M. Improving graph neural network expressivity via subgraph isomorphism counting. *arXiv preprint arXiv:2006.09252*, 2020.
- Coppersmith, D. L infinity embeddings. In *Approximation, Randomization, and Combinatorial Optimization: Algorithms and Techniques*, pp. 223–228. Springer, 2001.
- Devlin, J., Chang, M.-W., Lee, K., and Toutanova, K. Bert: Pre-training of deep bidirectional transformers for language understanding. *arXiv preprint arXiv:1810.04805*, 2018.
- Emek, Y., Pfister, C., Seidel, J., and Wattenhofer, R. Anonymous Networks: Randomization = 2-Hop Coloring. In *33rd ACM Symposium on Principles of Distributed Computing (PODC), Paris, France, July 2014*.
- Fout, A. M. *Protein interface prediction using graph convolutional networks*. PhD thesis, Colorado State University, 2017.
- Gilmer, J., Schoenholz, S. S., Riley, P. F., Vinyals, O., and Dahl, G. E. Neural message passing for quantum chemistry. In *International conference on machine learning*, pp. 1263–1272. PMLR, 2017.
- Gori, M., Monfardini, G., and Scarselli, F. A new model for learning in graph domains. In *Proceedings. 2005 IEEE International Joint Conference on Neural Networks, 2005.*, volume 2, pp. 729–734. IEEE, 2005.
- Hamilton, W. L., Ying, R., and Leskovec, J. Inductive representation learning on large graphs. In *Proceedings of the 31st International Conference on Neural Information Processing Systems*, pp. 1025–1035, 2017.
- Helfgott, H. A., Bajpai, J., and Dona, D. Graph isomorphisms in quasi-polynomial time. *arXiv preprint arXiv:1710.04574*, 2017.
- Henaff, M., Bruna, J., and LeCun, Y. Deep convolutional networks on graph-structured data. *arXiv preprint arXiv:1506.05163*, 2015.
- Irwin, J. J., Sterling, T., Mysinger, M. M., Bolstad, E. S., and Coleman, R. G. Zinc: a free tool to discover chemistry for biology. *Journal of chemical information and modeling*, 52(7):1757–1768, 2012.
- Junttila, T. and Kaski, P. Engineering an efficient canonical labeling tool for large and sparse graphs. In *2007 Proceedings of the Ninth Workshop on Algorithm Engineering and Experiments (ALENEX)*, pp. 135–149. SIAM, 2007.
- Kamada, T., Kawai, S., et al. An algorithm for drawing general undirected graphs. *Information processing letters*, 31(1):7–15, 1989.
- Kipf, T. N. and Welling, M. Semi-supervised classification with graph convolutional networks. *arXiv preprint arXiv:1609.02907*, 2016.
- Klemmer, K., Safir, N., and Neill, D. B. Positional encoder graph neural networks for geographic data. *arXiv preprint arXiv:2111.10144*, 2021.
- Krizhevsky, A., Sutskever, I., and Hinton, G. E. Imagenet classification with deep convolutional neural networks. *Advances in neural information processing systems*, 25: 1097–1105, 2012.
- Lewis, M., Liu, Y., Goyal, N., Ghazvininejad, M., Mohamed, A., Levy, O., Stoyanov, V., and Zettlemoyer, L. Bart: Denoising sequence-to-sequence pre-training for natural language generation, translation, and comprehension. *arXiv preprint arXiv:1910.13461*, 2019.
- Li, P., Wang, Y., Wang, H., and Leskovec, J. Distance encoding: Design provably more powerful neural networks for graph representation learning. *arXiv preprint arXiv:2009.00142*, 2020.
- Loukas, A. What graph neural networks cannot learn: depth vs width. *arXiv preprint arXiv:1907.03199*, 2019.
- Ma, L., Rabbany, R., and Romero-Soriano, A. Graph attention networks with positional embeddings. In *PAKDD (1)*, pp. 514–527. Springer, 2021.
- Maron, H., Ben-Hamu, H., Shamir, N., and Lipman, Y. Invariant and equivariant graph networks. *arXiv preprint arXiv:1812.09902*, 2018.
- Maron, H., Ben-Hamu, H., Serviansky, H., and Lipman, Y. Provably powerful graph networks. *arXiv preprint arXiv:1905.11136*, 2019.
- McKay, B. D. and Piperno, A. Practical graph isomorphism, ii. *Journal of symbolic computation*, 60:94–112, 2014.
- Morris, C., Ritzert, M., Fey, M., Hamilton, W. L., Lenssen, J. E., Rattan, G., and Grohe, M. Weisfeiler and leman go

- neural: Higher-order graph neural networks. In *Proceedings of the AAAI Conference on Artificial Intelligence*, volume 33, pp. 4602–4609, 2019.
- Papp, P. A., Martinkus, K., Faber, L., and Wattenhofer, R. DropGNN: Random Dropouts Increase the Expressiveness of Graph Neural Networks. *Advances in Neural Information Processing Systems*, 34, 2021.
- Rong, Y., Huang, W., Xu, T., and Huang, J. Dropedge: Towards deep graph convolutional networks on node classification. *arXiv preprint arXiv:1907.10903*, 2019.
- Sanchez-Gonzalez, A., Godwin, J., Pfaff, T., Ying, R., Leskovec, J., and Battaglia, P. Learning to simulate complex physics with graph networks. In *International Conference on Machine Learning*, pp. 8459–8468. PMLR, 2020.
- Sato, R., Yamada, M., and Kashima, H. Approximation ratios of graph neural networks for combinatorial problems. *arXiv preprint arXiv:1905.10261*, 2019.
- Sato, R., Yamada, M., and Kashima, H. Random features strengthen graph neural networks. In *Proceedings of the 2021 SIAM International Conference on Data Mining (SDM)*, pp. 333–341. SIAM, 2021.
- Scarselli, F., Gori, M., Tsoi, A. C., Hagenbuchner, M., and Monfardini, G. The graph neural network model. *IEEE transactions on neural networks*, 20(1):61–80, 2008.
- Shaw, P., Uszkoreit, J., and Vaswani, A. Self-attention with relative position representations. *arXiv preprint arXiv:1803.02155*, 2018.
- Shervashidze, N., Schweitzer, P., Van Leeuwen, E. J., Mehlhorn, K., and Borgwardt, K. M. Weisfeiler-lehman graph kernels. *Journal of Machine Learning Research*, 12(9), 2011.
- Veličković, P., Cucurull, G., Casanova, A., Romero, A., Lio, P., and Bengio, Y. Graph attention networks. *arXiv preprint arXiv:1710.10903*, 2017.
- Weisfeiler, B. and Leman, A. The reduction of a graph to canonical form and the algebra which appears therein. *NTI, Series*, 2(9):12–16, 1968.
- Xu, K., Hu, W., Leskovec, J., and Jegelka, S. How powerful are graph neural networks? *arXiv preprint arXiv:1810.00826*, 2018.
- Yanardag, P. and Vishwanathan, S. Deep graph kernels. In *Proceedings of the 21th ACM SIGKDD international conference on knowledge discovery and data mining*, pp. 1365–1374, 2015.
- Ying, R., He, R., Chen, K., Eksombatchai, P., Hamilton, W. L., and Leskovec, J. Graph convolutional neural networks for web-scale recommender systems. In *Proceedings of the 24th ACM SIGKDD International Conference on Knowledge Discovery & Data Mining*, pp. 974–983, 2018.

A. Proof of Theorem 3.1

Theorem A.1. *GINs of sufficient depth augmented with canonical node IDs can distinguish any two non-isomorphic graphs.*

The proof follows from Corollary 3.1 in (Loukas, 2019). First we state the corollary again for convenience:

Corollary 3.1. *GNN_{mp}^n can compute any Turing computable function over connected attributed graphs if the following conditions are jointly met: each node is uniquely identified; (MSG) and UP are Turing-complete for every layer; the depth is at least $d \geq D$ layers; and the width is unbounded.*

D denotes the diameter of the graph. GNN_{mp}^n refers to a general message passing GNN. (MSG) and UP are alternative characterizations of the AGGREGATE and UPDATE steps. The equivalence of the two models is shown in the paper. And GIN (with sufficient width and depth) is used an example of a network that satisfies the conditions of the theorem.

Proof. First note that if we can compute any Turing computable function over connected attributed graphs, then in particular we can also solve the graph isomorphism problem. So what remains to be shown is that GIN augmented with canonical node IDs satisfies the condition of the corollary. We already know that GIN with appropriate hyperparameters satisfies the conditions on the GNN. And finally, if we assign a canonical ID to each node, then each node is uniquely identified. \square

B. Proof of Theorem 3.2

Theorem B.1. *Every graph $G = (V, E)$ embeds isometrically into l_∞ .*

Proof. Let $V = \{v_1, v_2, \dots, v_n\}$. We define $f_i(v_j) = d(v_i, v_j)$, i.e., as the distance between nodes v_i and v_j in G , and we define the mapping of the nodes into l_∞ as:

$$f(v_j) = \begin{pmatrix} f_1(v_j) \\ \dots \\ f_n(v_j) \end{pmatrix}$$

Then by the triangle inequality, we have for any $k \in 1, 2, \dots, n$

$$|f_k(v_i) - f_k(v_j)| = |d(v_i, v_k) - d(v_k, v_j)| \leq d(v_i, v_j).$$

Therefore,

$$\|f(v_i) - f(v_j)\|_\infty \leq d(v_i, v_j).$$

And by construction, considering $k = i$ gives

$$\|f(v_i) - f(v_j)\|_\infty = \max_k |f_k(v_i) - f_k(v_j)| \geq |f_i(v_i) - f_i(v_j)| = f_i(v_j) = d(v_i, v_j).$$

Combining these we have

$$\|f(v_i) - f(v_j)\|_\infty = d(v_i, v_j).$$

\square

C. Proof of Theorem 3.3

Theorem C.1. *GIN of sufficient depth augmented with isometric l_∞ -embeddings can distinguish any two non-isomorphic graphs.*

Proof. The proof follows the same reasoning as the proof of Theorem A.1 above. What remains to be shown is that the l_∞ -embeddings we defined in the proof of Theorem B.1 are unique. However, this is trivial by construction, since for all $v_i, v_j \in V$, we have

$$\|f(v_i) - f(v_j)\|_\infty = d(v_i, v_j) \geq 0.$$

This of course holds for all isometric embedding, since the distance between any two nodes in an unweighted graph is always at least 1. \square

D. Synthetic Datasets

Here are the complete results for the synthetic datasets using GIN as the base GNN architecture. We include both test AUROC and test accuracy tables. Scores are always from the final epoch.

dataset	C3	C4	C5	C6	K4	K5	K6	LCC
model								
GIN	0.500000	0.500000	0.500000	0.500000	0.500000	0.500000	0.500000	0.500000
+ canon(1)	0.876214	0.633173	0.561823	0.566377	0.591223	0.563640	0.563415	0.725541
+ canon(20)	0.942873	0.605225	0.544443	0.559831	0.672548	0.594462	0.577431	0.842679
+ l_inf(20)	0.685647	0.597073	0.525939	0.547593	0.597704	0.561581	0.536033	0.701265
+ pos(2)	0.967564	0.909830	0.763035	0.723195	0.780109	0.750997	0.751688	0.880379
+ pos(2)+rBits(1)	0.968063	0.910487	0.772632	0.721797	0.783297	0.755356	0.758229	0.884294
rUniform	0.912876	0.674531	0.592948	0.597580	0.551445	0.519268	0.513956	0.685899
rNormal(1)	0.898043	0.651839	0.586708	0.609292	0.553445	0.511766	0.508493	0.684939
rBits(2)	0.948913	0.700615	0.612436	0.621742	0.546305	0.506981	0.514774	0.694703

Figure 7. AUROC scores on the synthetic tasks using GIN with 5 layers as the base GNN model.

dataset	C3	C4	C5	C6	K4	K5	K6	LCC
model								
GIN	0.218850	0.618300	0.388800	0.832850	0.561550	0.509000	0.592750	0.401550
+ canon(1)	0.835100	0.606600	0.560700	0.721400	0.570050	0.545100	0.554250	0.487500
+ canon(20)	0.910050	0.603350	0.556650	0.769550	0.624850	0.559650	0.544800	0.657450
+ l_inf(20)	0.648100	0.599400	0.539600	0.752900	0.558500	0.543500	0.505000	0.483950
+ pos(2)	0.942450	0.844450	0.711500	0.786400	0.720650	0.688450	0.699600	0.699550
+ pos(2)+rBits(1)	0.943000	0.851050	0.720300	0.781950	0.722750	0.692550	0.709550	0.709350
rUniform	0.807600	0.615100	0.558450	0.608800	0.549100	0.512150	0.550750	0.397750
rNormal(1)	0.797650	0.599250	0.564600	0.621500	0.553450	0.505850	0.549350	0.390400
rBits(2)	0.856950	0.638700	0.573200	0.618000	0.537050	0.499450	0.538850	0.399100

Figure 8. Test accuracies on the synthetic tasks using GIN with 5 layers as the base GNN model.

Here are the complete results for the synthetic datasets using GCN as the base GNN architecture. We include both test AUROC and test accuracy tables. Scores are always from the final epoch.

GNNs with Precomputed Node Features

dataset	C3	C4	C5	C6	K4	K5	K6	LCC
model								
GCN	0.500000	0.500000	0.500000	0.500000	0.500000	0.500000	0.500000	0.500000
+ canon(20)	0.960170	0.614048	0.559783	0.574503	0.707117	0.625519	0.623023	0.816392
+ pos(2)	0.949968	0.872787	0.756127	0.731384	0.802407	0.771112	0.786754	0.868566
+ pos(2)+rBits(1)	0.949306	0.864142	0.748409	0.733248	0.809367	0.782131	0.793915	0.873339
rUniform	0.801317	0.629058	0.572320	0.586304	0.525416	0.520859	0.489023	0.639837
rBits(2)	0.853689	0.639008	0.569820	0.622825	0.531696	0.517305	0.490952	0.647672

Figure 9. AUROC scores on the synthetic tasks using GCN with 5 layers as the base GNN model.

dataset	C3	C4	C5	C6	K4	K5	K6	LCC
model								
GCN	0.791250	0.618300	0.388800	0.832850	0.438450	0.491000	0.592750	0.401550
+ canon(20)	0.914700	0.607850	0.563500	0.760450	0.655350	0.586350	0.577600	0.633350
+ pos(2)	0.913300	0.808200	0.699350	0.717250	0.742600	0.704150	0.723600	0.658800
+ pos(2)+rBits(1)	0.902000	0.799950	0.695100	0.713900	0.751100	0.716050	0.728050	0.669100
rUniform	0.721400	0.573050	0.560650	0.600000	0.511250	0.515600	0.562800	0.349800
rBits(2)	0.751300	0.582000	0.553800	0.605250	0.525300	0.515400	0.557400	0.353050

Figure 10. Test accuracies on the synthetic tasks using GCN with 5 layers as the base GNN model.

E. Further Experiments

E.1. Canon has better learning efficiency

In terms of the test AUROC, canon and pos models level out at around the same time, at epoch 100, but the pos model at a higher value. The models with the random augmentations level off much later, after epoch 250.

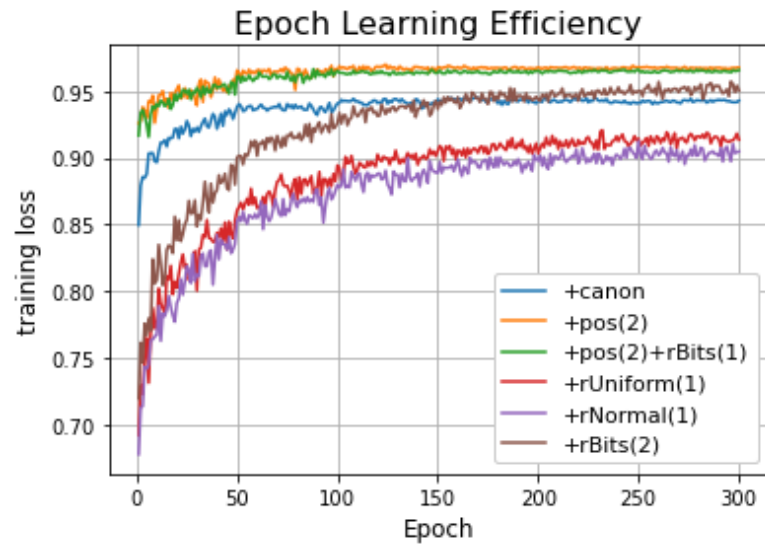


Figure 11. Weighted test AUROC over the first 300 epochs on C3.